13th International Conference on
Structural Health Monitoring of Intelligent Infrastructure
DOI: 10.3217/978-3-99161-057-1-154

Optimizing Bridge Recalculation: Uncertainty in SHM-Based Recalculation of Prestressed Concrete Bridges

Maria Walker[1], Cedric Eisermann[1], Jan-Hauke Bartels[2], Steffen Marx[1]
[1]Institute of Concrete Structures, Faculty of Civil Engineering, TUD Dresden University of Technology, George-Bähr-Str. 1, 01069 Dresden, Germany
[2]LPI Ingenieurgesellschaft mbH, Völgerstraße 9, 30519 Hannover, Germany
email: maria.walker1@tu-dresden.de, cedric.eisermann@tu-dresden.de, bartels@lpi-ing.de, steffen.marx1@tu-dresden.de

ABSTRACT: There are several ways to incorporate SHM data into the structural assessment of existing bridges. Beyond conventional model calibration, SHM can improve environmental effects and load estimates, thereby reducing the model uncertainty. However, the measurement data itself is also affected by epistemic uncertainty. This paper investigates the influence of selected data quality characteristics on the recalculation of prestressed concrete bridges, focusing on the example of coupling joints. A research bridge serves as a case study, equipped with temperature sensors recording data since February 2024 until today. A numerical FE model of the bridge provides a solid basis for simulations. A sensitivity analysis was carried out to identify the key parameters influencing the results. This includes the effect of the temperature gradient on the fatigue stress of the coupling joint. The study demonstrates the impact of representativeness and coverage of measurements in a spatial and temporal context on the estimated remaining service life of the structure. It highlights the importance of the correct selection of the sensor number and placement, and of the data collection period length. The results confirm the suitability of the proposed methodology for the systematic evaluation of monitoring concepts. However, further research is needed to derive specific recommendations for the design of monitoring systems for coupling joints. This work contributes to optimized SHM-based bridge recalculation by providing a basis for assessing the quality of monitoring concepts and its influence on structural analysis.

KEY WORDS: Sensitivity analysis; Measurement uncertainty; Fatigue; Coupling joints; Temperature monitoring.

1 INTRODUCTION

A large number of bridges on Germany's federal highways were built in the 1960s and 1970s (see Figure 1) and have been exposed for more than 55 years to heavy traffic and other loads, for which they were not initially designed. About 47 % of these bridges are prestressed concrete bridges [1]. In addition to durability and overloading issues, fatigue is an important concern for many of these structures [2].

Figure 1. Bridge age along German federal highways, [1].

Long-span prestressed concrete bridges are typically constructed by concreting in sections (see Figure 2). Each section is prestressed as a partial structure to avoid the accumulation of frictional losses over the length of the superstructure. Each new section is prestressed against the previous one. The tendons are connected at the coupling joints by coupler anchors. One half of the fixed coupler anchor is embedded in the concrete of the previous section and serves as the end anchorage during the construction of this section. The other half of the anchor is located in the new section (see Figure 2). The tendons are then connected by tying the tendons of the next section to the coupler anchor already embedded in the concrete [3].

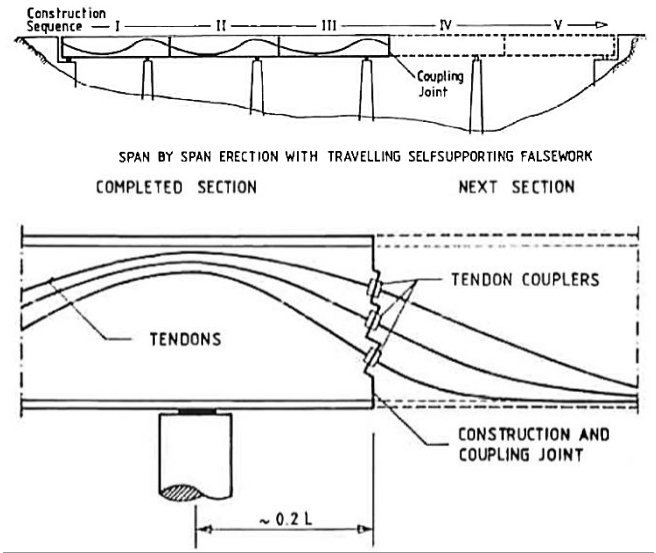

Figure 2. Section-by-section construction of a prestressed concrete bridge and a historical construction detail of a coupling joint, [4].

The first case of fatigue failure to coupler joints – and the only known fatigue failure to date – occurred in 1976 in the bridge “Hochstraße Prinzenallee” in Düsseldorf, Germany. This incident led to extensive theoretical and experimental research

DOI: 10.3217/978-3-99161-057-1-154

[5; 6] as well as to the complementation of the technical rules for coupling joints in Germany. These regulations include the calculation of fatigue resistance, the more precise assessment of internal forces, and new design regulations. As a result of these regulations, it can generally be assumed that the coupling joints constructed from 1979 have no fatigue deficits [7]. The following causes of damage in coupling joints (vertical cracks and fatigue of tendons) were identified [3; 8; 9]:

- Concrete tensile strength in the joint is negligible;
- Neglect of temperature gradient over the height in the design stage;
- Position close to the points of contraflexure, where the temperature effects, and the scattering of the dead loads are important factors to consider;
- Non-linear strain distribution due to sectional prestressing;
- Internal stress states due to hydration heat;
- Increased prestressing losses in the coupling joint because of creep, shrinkage, and prestressing steel relaxation (CSR) due to the larger geometry of the couplers;
- Reduced fatigue strength of the tendons in the coupling joint due to fretting corrosion;
- Uneven distribution of tendons across the cross-section.

Consequently, infrastructure operators have routinely carried out recalculations of existing bridges based on advanced standards and guidelines. The recalculation guideline for existing road bridges [10] plays a key role in this context. After the introduction of this guideline in 2011, the results of the first recalculations were systematically evaluated in a research project on behalf of the Federal Highway and Transport Research Institute [11]. In this study, 43 % of the 126 investigated prestressed structures showed a calculational fatigue deficit at the coupling joints. This makes the fatigue verification of coupling joints the second most frequent failure mechanism that leads to calculational deficits. The recent evaluation of recalculations [7] took into account the first supplement to the recalculation guideline from 2015 [12]. The coupling joint fatigue was recalculated for 63 bridges, of which 33 showed deficits. In 37 % of the recalculations with coupling joint deficits, the fatigue resistance was exceeded by more than 50 % [7], see Figure 3.

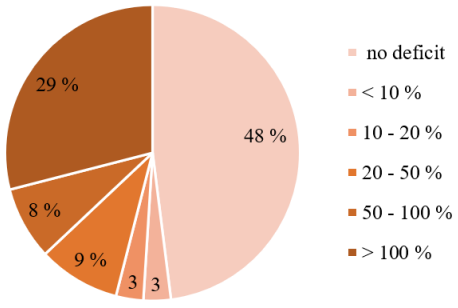

Figure 3. Fatigue deficits for coupling joints according to the German recalculation guideline after 2015, [7].

These calculational deficits do not necessarily indicate actual structural damage. However, they often lead to expensive external post-tensioning or even to a premature demolition of a bridge before the end of its intended service life. To improve the assumptions about the actual impacts and resistances, the use of monitoring data is a powerful tool. The objective of monitoring is to reduce epistemic uncertainty, which arises from incomplete knowledge and can be reduced by increasing the amount of information or improving the model quality. In contrast, aleatory uncertainty – reflecting inherent randomness such as signal noise – is considered irreducible and is typically modeled stochastically [13–15]. In structural safety assessment, conservative assumptions are generally applied. Therefore, reducing epistemic uncertainty through monitoring data is expected to have a beneficial effect on the estimated load-bearing capacity and the predicted service life of the structure. This is especially true for bridges with high traffic volumes that exhibit considerable temporal variations in load, where incorporating measured daily temperature and traffic loads can yield more accurate results [16].

However, monitoring methods applied in practice are highly heterogeneous, with no standardized guidelines for the design of measurement systems, data evaluation, or data integration in the measurement-based recalculation. Standards for data quality requirements and quantifiable quality indicators are also missing. Consequently, monitoring concepts are often based on empirical knowledge, and the assessment of data quality remains subjective. The quality of the monitoring concept directly influences the quality of the resulting monitoring data, which in turn affects the reliability of structural condition assessments. Therefore, it is essential to consider both the data quality and the quality of the monitoring concept itself.

This paper presents a systematic methodology for the evaluation of an existing temperature monitoring concept, with regard to selected quality characteristics and their impact on the recalculation results using coupling joints as an example.

2 TEMPERATURE MONITORING FOR BRIDGE ASSSESSMENT

The relationship between the bending moment M and the prestressing steel stress σ_P is described by the moment-stress diagram. The normal force, prestressing force, geometry of the cross section, material stiffness and tendon distribution influence the position and shape of the moment-stress curve, which is shown in Figure 4. It consists of three sections [17]:

- Linear-elastic behavior in uncracked state (Mode I)
- Transition area with concrete tensile strength f_{ct} = 0 N/mm²
- Distinct cracked state (Mode II).

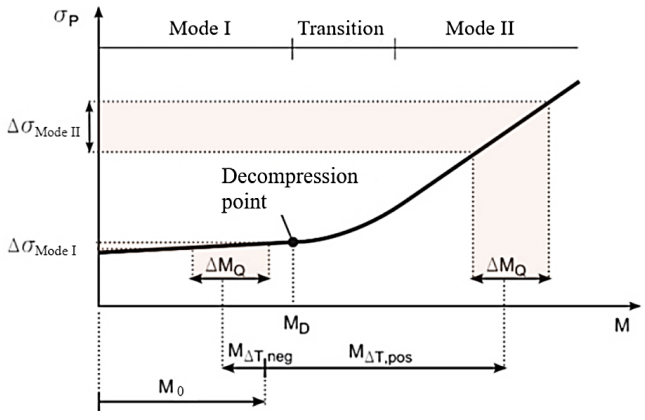

Figure 4. Moment-stress diagram for prestressing steel, [3].

DOI: 10.3217/978-3-99161-057-1-154

In addition to the alternating moment ΔM_Q due to traffic impact, the so-called base moment M_0 has a substantial influence on the stress range $\Delta\sigma_P$. The base moment M_0 is caused by the following components: dead weight of the structure, statically indeterminate part of the prestressing, losses due to CSR, redistributions from the construction to the final state, settlements as well as temperature loads. As long as the structure remains in Mode I, the stress range $\Delta\sigma_{\text{Mode I}}$ is relatively low. However, once the decompression point is exceeded ($M > M_D$) and the upper stress enters Mode II, fatigue-relevant stress ranges $\Delta\sigma_{\text{Mode II}}$ are expected. The stress range $\Delta\sigma_P$ in Mode II is considerably higher than in Mode I, despite the same impact through ΔM_Q. The increase in the base moment M_0 required for the Mode II can be caused, for example, by large vertical temperature gradients $M_{\Delta T,pos}$ or prestressing losses [8]. For coupling joints, the moment component induced by temperature gradients is decisive in comparison to permanent loads, as they are typically located close to the points of contraflexure (points of zero bending moment). For older existing structures, variations of the base moment depend primarily on the temperature gradient, as redistributions, settlements and CSR are already completed [9].

For the reasons stated above, fatigue calculation of prestressed concrete bridges requires, in addition to the stress range $\Delta\sigma$ in the prestressing steel from the traffic load ΔM_Q, the knowledge of the magnitude of the base moment M_0. Therefore, the stress range monitoring in coupling joints is usually combined with temperature measurements. The temperature load $M_{\Delta T}$ is a non-stationary variable influenced by environmental factors. While solar radiation and air temperature determine the general thermal input, wind speed and humidity affect the rate of heat exchange between the structure and the surrounding air. Additionally, the geographical orientation of the structure, height above ground, pavement thickness and other factors affect the temperature load [16].

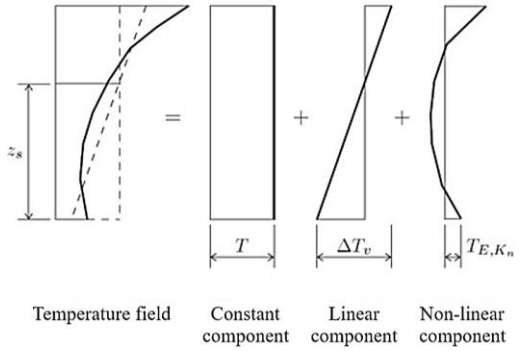

Figure 5. Temperature field components, [16].

The temperature field of a bridge cross-section can be divided into three components (Figure 5): (1) *The constant component* T induces no internal forces or stresses if the deformation of the structure is not impeded. (2) *The linear component* ΔT_y causes a curvature that creates a constraining moment if the deflection is impeded. This component results in internal forces and therefore stresses in the cross-section. Only this component is considered in fatigue recalculations of coupling joints. (3) *The non-linear component* T_E is usually neglected in calculations of stresses [18].

In order to capture the linear temperature gradient over the entire cross-section, it is necessary to suitably distribute temperature sensors over the cross-section und to choose an appropriate monitoring period [16]. According to [2; 19], a measurement period of a whole year is sufficient to determine the structure-specific temperature load in the coupling joint. However, for Germany, the measurement period can be reduced to 3 to 6 months during the summer months (May to August), as both the highest positive and negative temperature gradients occur during this period [18]. Winter months are unsuitable for monitoring due to the low intensity of solar radiation. High gradients are especially observed when a cool, cloudy period is followed by a sunny day [9]. In [20] on the basis of measurements on a bridge and in [18] on the basis of simulation calculations, it was determined that the greatest temperature changes over the cross-sectional height occur in

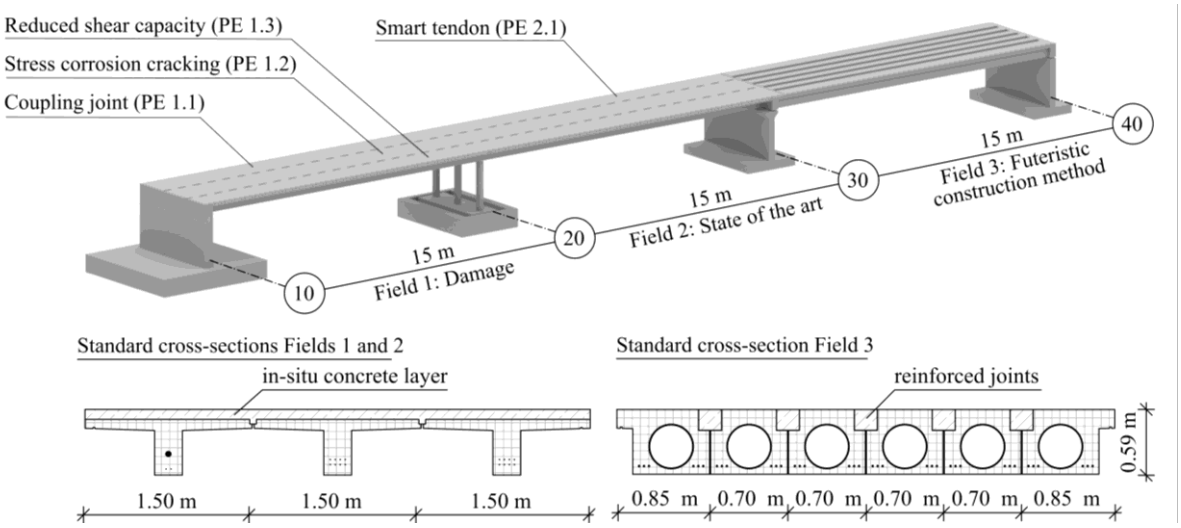

Figure 6. Illustration of the openLAB bridge including the standard cross-sections (Graphic: Fabian Collin, Max Herbers).

DOI: 10.3217/978-3-99161-057-1-154

the slab, which requires a denser arrangement of temperature sensors in this area than in the webs.

The following section presents the existing measurement concept for recording temperature effects on a demonstrator structure – the openLAB research bridge located in Germany.

3 CASE STUDY: RESEARCH BRIDGE OPENLAB

3.1 The structure and its coupling joint

The reference structure openLAB is a 45-meter-long and 4.5-meter-wide prestressed concrete bridge located in Bautzen, Germany. Constructed as part of the research project IDA-KI, it serves as a large-scale demonstrator for advancing structural health monitoring (SHM) and digital twin technologies. The bridge comprises three 15-meter spans, each meticulously designed to address specific research objectives [21].

Spans 1 and 2 consist of three precast elements (PE) with T-shaped cross-sections, which are transversely connected by a cast-in-place concrete layer, see Figure 5. Span 1 has been designed to replicate typical structural deficiencies of early tensioning methods, such as coupling joint problems, stress corrosion cracking, and areas with reduced shear capacity. Span 2 represents state-of-the-art construction methods and integrates innovative "smart tendons" which are equipped with integrated distributed fiber optic sensors [22]. Span 3 showcases a prefabricated construction system that eliminates the need for cast-in-place concrete. This system employs hollow precast elements that are transversely coupled by grouting joints, enabling the PE to be fully loadable immediately after installation.

All PEs are prestressed with strands that have an immediate bond. In addition, PE 1.1 and 2.1 are post-tensioned (see Figure 6 and Figure 7). The structural system features monolithic connections between the superstructure and substructure at axes 10 and 20. At axis 30, a connection between spans 2 and 3 with ultra-high-performance fiber-reinforced cementitious composite material (UHPFRC) is planned. However, the connection will be implemented at a later stage, after the first load tests planned for May 2025. Currently, span 3 remains statically decoupled from the other two spans.

The coupling joint under investigation is situated in PE 1.1, at the estimated point of contraflexure. The PE was constructed in multiple stages. Initially, a 4-meter segment of the element was fabricated and partially post-tensioned. Subsequently, the remaining 11-meter segment was cast, which also included the partial prestressing of the second tendon. The connection between the first and second tendons was achieved using a fixed coupler, certified under European Technical Assessment No. 13/0839. The first tendon was anchored in a manner consistent with the use of an anchor head for stressing anchors. In addition to a stress anchor, the coupler head provides a projecting ring collar with slots. The prestressing steel strands of the second tendon were placed in the slots and secured with a tensioning belt. Following this, the strands in immediate bond were prestressed, and the tendons in subsequent bond were tensioned to their final prestressing force. Finally, the tendon ducts were grouted to ensure proper bonding and corrosion protection of the prestressing steel.

3.2 Temperature monitoring of openLAB

A comprehensive monitoring system has been installed at the openLAB since "hour zero" – the beginning of the construction phase. This monitoring system integrates global and local measurement techniques, providing detailed insights into the bridge's structural behavior and environmental influences. Acceleration, inclination, and displacement sensors are employed to assess global structural behavior. Concurrently, environmental parameters such as air temperature, relative humidity, solar radiation, and precipitation are continuously recorded to account for external influences. Local measurements, in contrast, target areas susceptible to structural damage. These include strain gauges on reinforcement bars, distributed fiber optic sensors (DFOS) embedded in the concrete, and linear displacement transducers to monitor crack widths, e.g., in the coupling joint.

The component temperature is measured using temperature sensors, which were embedded into the PE 1.1 near the coupling joint during the construction phase. There are three temperature sensors (PT100) distributed over the height (see Figure 7). These sensors have been continuously recording data at 10-minute intervals since February 2024 until today.

To assess the influence of temperature measurement uncertainty on the recalculation results for the coupling joint, temperature data recorded by the component temperature sensors between January 31, 2024, and February 28, 2025, at 10-minute intervals, was used to calculate the linear temperature gradient. A reference dataset – Test No. 0.1 – was defined by using the full observation period (January 2024 to February 2025), a sampling interval of 10 minutes, and the complete sensor configuration including all three temperature sensors: T_{top}, T_{middle}, and T_{bottom}.

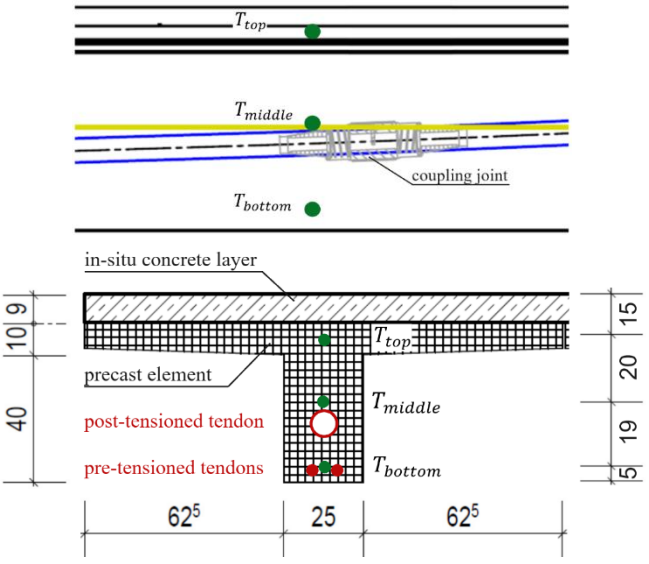

Figure 7. Installed temperature sensors embedded in the PE 1.1 of openLAB; all measures are given in cm.

The linear temperature gradient $\Delta T_{M,y}$, which induces a bending moment M_y in the coupling joint under consideration, is calculated using the following equation [23]:

$$\Delta T_{M,y} = \frac{h}{I_y} \cdot \sum_{i=1}^{n} T_i \cdot S_{y,i} \qquad (1)$$

DOI: 10.3217/978-3-99161-057-1-154

In this formulation, h denotes the total cross-sectional height, I_y is the second moment of area about the y-axis, T_i represents the temperature at a specific sub-area of the cross-section, and $S_{y,i}$ is the first moment of area of the respective sub-area. The cross-section is conceptually discretized into n small sub-areas. The temperature values between the fixed-position sensors (T_{top}, T_{middle}, and T_{bottom}) are linearly interpolated or extrapolated to estimate the temperature distribution throughout the height of the cross-section. This approach is not limited to the number of available sensors but rather assumes a continuous distribution of temperature across the section.

3.3 Fatigue simulation

The residual fatigue life is predicted based on the accumulated fatigue damage D. Failure occurs at $D = 1$. The fatigue damage is calculated according to Miner's rule [24]:

$$D = \sum_{i=1}^{m} D_i = \sum_{i=1}^{m} \frac{n(\Delta\sigma_i)}{N(\Delta\sigma_i)} \leq 1 \qquad (2)$$

The damage at a load level i is derived from the ratio of applied load cycles n to bearable load cycles N. The load cycles until failure are obtained from the S-N curve (Wöhler curve) according to the stress range $\Delta\sigma_i$. The progression of fatigue damage is simplified through extrapolation of the frequency of calculated stress ranges $\Delta\sigma_i$ from varying traffic and temperature loads.

For traffic loads, the fatigue load model FLM 4, as defined by EN 1991-2, was applied. It consists of five standardized truck types which represent the characteristics of heavyweight traffic in Europe. To achieve relevant stress states up to the ultimate limit state with reasonable testing effort, only 25 % of Load Model 1 according to EN 1991-2 was considered for the design of the openLAB. Consequently, FLM 4 was appropriately scaled to ensure realistic stress amplitudes. Relevant load positions for the truck types were determined using influence lines.

For temperature loads, both the temperature gradients from the recalculation guideline and the temperature gradients from structural monitoring are considered (see Section 4.1).

The annual damage contribution D_{year} is calculated as the sum of partial damages $D_{\Delta T,i}$, incurred during the passage of a standard vehicle of type i under the simultaneous action of the temperature gradient ΔT. The index $i = 1\ldots5$ covers the five vehicle types according to the FLM 4. Only high temperature gradients combined with heavy traffic lead to fatigue damage. The partial damage is weighted according to the relative frequency of individual vehicle types p_i in the annual traffic volume N_{obs} and the annual probability of occurrence of the temperature gradient $\lambda_{T,\Delta T}$:

$$D_{year} = N_{obs} \cdot \sum_{\Delta T=\min \Delta T}^{\max \Delta T} \left[\sum_{i=1}^{5} p_i \cdot \lambda_{T,\Delta T} \cdot D_{\Delta T,i} \right] \qquad (3)$$

The calculation of internal forces in the cross-section of the coupling joint was performed using a linear-elastic finite element (FE) model developed in SOFiSTiK (version 2024). Given the complete decoupling of spans 1 and 2 from span 3, the structural model was simplified to a two-span system. The T-beams were modeled using beam elements with six degrees of freedom per node (three translations and three rotations). In the transverse direction, the three parallel beam axes were coupled using plate elements (see Figure 8).

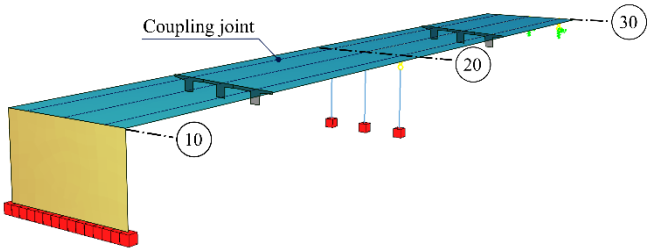

Figure 8: FE-Model of openLAB.

To accurately represent the load-bearing behavior of the integral structure, the abutment wall at axis 10 and the columns at axis 20 were modeled and rigidly coupled with the superstructure. Shell elements (abutment wall) and beam elements (columns) were used to idealize the substructures. At axis 30, the superstructure is supported on the substructure via a hinged connection. Thus, the pier wall at the support point was simplified using equivalent, linear-elastic springs. The tendons were integrated into the FE model according to their position in the construction plans. Prestressing forces were calculated internally by SOFiSTiK and automatically applied to the intersected beam elements.

The structure was erected in various consecutive construction stages, which include the following: (1) manufacturing of the PEs in the factory; (2) construction of the substructures using cast-in-place concrete construction; (3) installation of PEs on temporary supports; and (4) production of the cast-in-place concrete layer for force-fit connection of PEs. The redistribution effects associated with this construction method, resulting from creep and shrinkage after the completion of the cast-in-place concrete addition, were accounted for in the FE model through different construction phases.

The calculation of the stress amplitudes $\Delta\sigma_i$ were performed for the relevant cross-section also in SOFiSTiK, considering the non-linear stress-strain relationships of concrete and steel.

4 IMPACT OF DATA QUALITY ON FATIGUE ASSESSMENT

4.1 Methodology

The collected measurement data only represents a sample from a total population. In this paper, three quality indicators were identified for the description of this property of measurement data at different levels: representativeness, coverage, and completeness. These quality indicators (for definition see Table 1) were originally presented by [25] for atmospheric measurements and adopted in the draft of VDI Guideline 3786 Sheet 1 [26]. These characteristics are adapted for the bridge monitoring and applied to the monitoring data of openLAB.

Completeness can be easily calculated as a percentage of the actual measurement data points relative to the expected measurement data points. This quality characteristic can be used to identify potential failures in the measurement system. In contrast, the other two quality characteristics – coverage and

DOI: 10.3217/978-3-99161-057-1-154

representativeness – cannot be described with a simple formula and should already be considered when designing the measurement system. Therefore, the two characteristics – coverage and representativeness – are the subject of the following considerations.

Table 1. Quality characteristic for data of atmospheric measurements, [25; 26].

Quality characteristics	Definition according to [25; 26]
Representativeness	The ability of a series of observations to provide an unbiased estimate of a parameter of a specified statistical population.
Coverage	Spatial and/or temporal distribution of measurement locations in the area under investigation.
Completeness	The extent to which the information provided enables the data user to draw conclusions in accordance with the goal and scope definition.

Table 2 provides an overview of the definitions of these quality characteristics for bridge monitoring. Spatial representativeness refers to the areas of the bridge structure where sensors are installed. The temporal representativeness describes the period during which the data is collected. Spatial coverage describes the number of sensors distributed within the representative area of the structure and whether sufficient metrological redundancy is achieved. Temporal coverage refers to the sampling frequency of the measurements.

Table 2. Quality characteristics for bridge monitoring concepts.

Quality characteristics	Definition for bridge monitoring
Representativeness	Spatial: Local distribution of sensors
	Temporal: Period of data collection
Coverage	Spatial: Sensor density
	Temporal: Sampling frequency

Insufficient monitoring data completeness affects the coverage, which in turn affects the representativeness of the data. Furthermore, incorrect selection of monitoring areas and periods can render the monitoring results unusable for the intended use case, even if coverage and completeness are high. To address this problem, this paper presents a methodology using the openLAB research bridge as a case study. This methodology can be applied to identify sufficient representativeness and coverage of monitoring data.

The spatial representativeness is investigated by varying the local distribution of the sensors in the upper and lower area of the cross-section. To assess the temporal representativeness, the observation period for the temperature measurements at openLAB was systematically varied between two days and a whole year. Spatial coverage was analyzed by altering the number of sensors, while temporal coverage was assessed by applying different sampling frequencies. A total of four test series were conducted in which only one of these three boundary conditions – observation period, sampling interval, sensor density, or local sensor distribution, – was varied at a time, while the others were held constant. This methodology corresponds to the one-at-a-time sensitivity analysis. The definition of the investigated test series is shown in Table 3.

Table 3. Definition of investigated test series.

No.	Description	Specification	
0.0	Recalculation guideline	-	
0.1	Reference measurement	12 months;	3 sensors
1.2	April – September	6 months;	3 sensors
1.3	May – August	4 months;	3 sensors
1.4	May – July	3 months;	3 sensors
1.5	June – July	2 months;	3 sensors
1.6	June	1 month;	3 sensors
1.7	08.07. – 09.07.2024	2 days;	3 sensors
2.2	0.00028 Hz (every hour)	12 months;	3 sensors
2.3	0.00002 Hz (every 12 hours)	12 months;	3 sensors
2.4	0.00001 Hz (every 24 hours)	12 months;	3 sensors
3.2	Upper and lower sensor	12 months;	2 sensors
4.2	Upper and middle sensor	12 months;	2 sensors
4.3	Middle and lower sensor	12 months;	2 sensors

Test Series 1 examines the impact of the temporal representativeness by shortening the observation period to six months (April - September 2024), four months (May - August 2024), three months (May - July 2024), two months (June - July 2024), one month (June 2024), and finally two days (July 8 - 9, 2024). The two-day period was selected according to the criteria that a cloudy day was followed by a sunny day [9]. This ensured a strong increase in air temperature and solar radiation within the observation period (Figure 9), which is expected to lead to high temperature gradients in the structure.

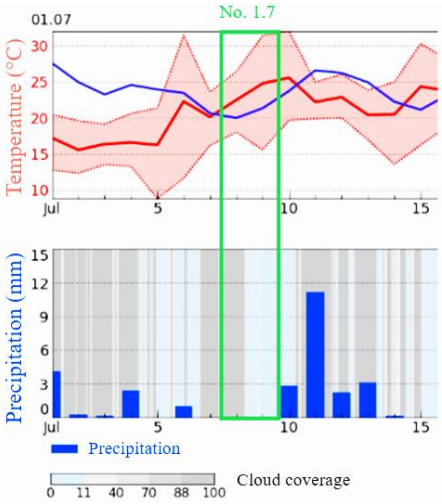

Figure 9. Meteorological data for the location Bautzen, Germany for the period from July 1st to July 15th 2024, [27].

Test Series 2 investigates the influence of the temporal coverage, i.e., sampling interval, by increasing it from the reference value of 10 minutes to 60 minutes, 720 minutes, and 1440 minutes.

Test Series 3 examines the effect of spatial coverage. In addition to the reference case using all three sensors (T_{top}, T_{middle}, T_{bottom}), this scenario considers only two sensors:

DOI: 10.3217/978-3-99161-057-1-154

T_{top} and T_{bottom}. Due to the limited number of installed sensors, only one variation of spatial coverage was possible.

Test Series 4 addresses the spatial representativeness in two scenarios with two sensors each: T_{top} and T_{middle}, and T_{middle} and T_{bottom}, with the objective of concentrating the sensors primarily at the bottom or top of the cross-section.

The probability distributions for the temperature gradients were determined according to the methodology presented in Section 3.2. The results of the parameter study for the calculation of the linear temperature gradient $\Delta T_{M,y}$ are illustrated in Figure 10. The linear temperature gradient determined for the openLAB is presented as a histogram of relative frequency f over $\Delta T_{M,y}$ for each test case. The reference case exhibits an approximately normal distribution, whereas, for example, Test 1.7 (observation period from July 8 to July 9, 2024) shows a notable deviation from normality due to the limited number of temperature readings. Other histograms reveal distributions with varying degrees of positive or negative skewness when compared to the reference distribution.

In the next step of the analysis, these histograms derived from real-world temperature measurements will be used to estimate the remaining service life of the openLAB structure according to the Section 3.3.

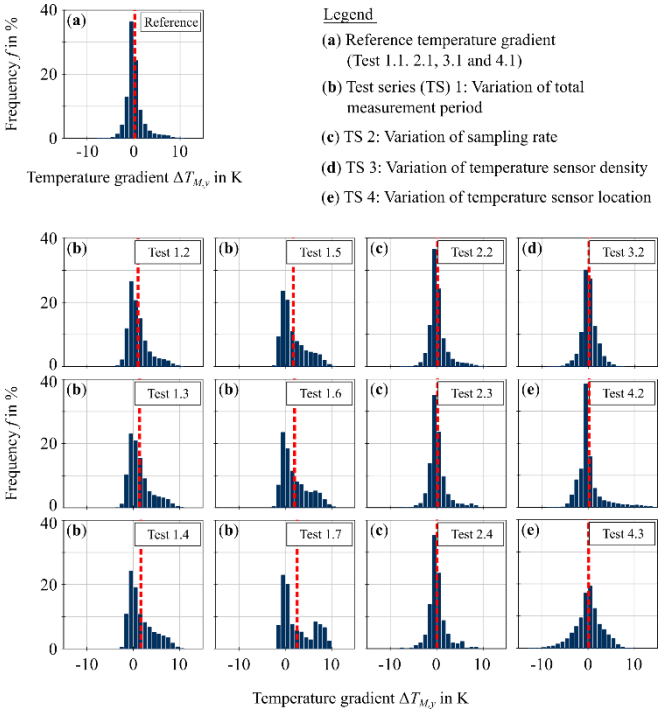

Figure 10. Parameter study on the influence of temperature measurement uncertainty on the linear temperature gradient. (**a**) Reference distribution; (**b**) Test series 1: Variation of total measurement period; (**c**) Test series 2: Variation of sampling rate; (**d**) Test series 3: Variation of temperature sensor density; (**e**) Test series 4: Variation of temperature sensor location.

In the German recalculation guideline [10], the temperature gradients are calculated in accordance with the reference standards DIN FB 101 and Eurocode DIN 1991-1-5. In addition, probabilities of occurrence for temperature gradients are specified for the calculation with the fatigue load model FLM 4. The guideline states temperature gradients to be applied according to the probability of occurrence and the cross-sectional shape of the bridge (box girder, T-beam, or slab) for a pavement thickness of 50 mm. The probabilities of occurrence for the temperature gradients were determined based on extensive investigations in [16]. For this purpose, hourly weather data were collected over eight years for three typical bridge cross-sections and evaluated statistically. The distribution and the daily course of the temperature load given in the German recalculation guideline were derived from this data. This standardized probability distribution is compared to the bridge-specific measurements of openLAB in Section 4.2. This comparison enables a quantification of the uncertainty in $\Delta T_{M,y}$ and its impact on the total service life assessment of the openLAB bridge.

4.2 Results

The results of the temperature gradient evaluation and the recalculation of the total service life for the coupling joint fatigue are summarized in Table 4. The first column corresponds to the test number. Test No. 0.0 represents the normative distribution given in the recalculation guideline, while No. 0.1 corresponds to the reference distribution, for which the entire temperature data set was utilized. The second and third columns contain the mean values μ and the values of the standard deviation σ of the temperature gradients ΔT in Kelvin. The third column provides the total service life in years for the respective data set about fatigue in the coupling joint. The last column shows the relative deviation of the service life compared to the reference distribution No. 0.1 in percent.

Table 4. Results of fatigue calculation.

No.	μ of ΔT in Kelvin	σ of ΔT in Kelvin	Absolute service life in years	Relative deviation of service life in %
0.0	1.800	± 2.619	1077.583 (recalculation guideline)	+ 7.69
0.1	0.198	± 1.887	**1000.634 (reference)**	-
1.2	0.983	± 2.289	1051.303	+ 5.06
1.3	1.357	± 2.463	1075.903	+ 7.52
1.4	1.625	± 2.698	1092.141	+ 9.14
1.5	1.720	± 2.731	1098.567	+ 9.79
1.6	2.013	± 2.873	1117.958	+ 11.72
1.7	2.546	± 3.334	1147.002	+ 14.63
2.2	0.198	± 1.887	1000.509	– 0.01
2.3	0.176	± 1.954	998.609	– 0.20
2.4	0.082	± 1.926	992.569	– 0.08
3.2	0.184	± 1.633	1001.866	+ 0.12
4.2	0.220	± 2.820	989.575	– 1.11
4.3	0.146	± 2.839	985.031	– 1.56

Overall, the variations in the measured data result in only minor deviations in the service life, which was determined to be approximately 1045 years on average for all test series. The service life that was calculated on the basis of the reference configuration gave a result of approximately 1001 years. Relative values range from – 1.56 % to + 14.63 %. This observation indicates that the impact of the temperature

DOI: 10.3217/978-3-99161-057-1-154

measurement uncertainty may not be a relevant factor for this structure with a relatively moderate influence on the fatigue of the coupling joint. The identification of relevant influence factors on the fatigue of the openLAB bridge will be systematically investigated in the further course of this study using a sensitivity analysis. It will enable a comparison of temperature influences with other relevant factors such as variation of traffic loads, prestressing losses or material properties.

It can be seen that the probability distribution of the temperature gradients from the recalculation guideline No. 0.0 leads to a slight overestimation of service life (+ 7.69 %) compared to the reference distribution No. 1.1 based on the complete measurement temperature data. In test series 1.2 to 1.7, in which the recording period becomes progressively shorter, there is a shift in the mean value towards high gradients and an increase in the standard deviation. Contrary to the expectation that this temperature gradient distribution would result in a reduced service life of the bridge, it continues to increase. This finding contradicts the information available in the literature (e.g. [9; 18; 20]), where the more frequent occurrence of positive temperature gradients (i.e., shorter measurement period in the summer months) normally leads to shorter service life. This unusual observation can be attributed to the initial stress state of the structure. Prestressing generates high negative bending moments in the coupling joint of the openLAB bridge (see Figure 11).

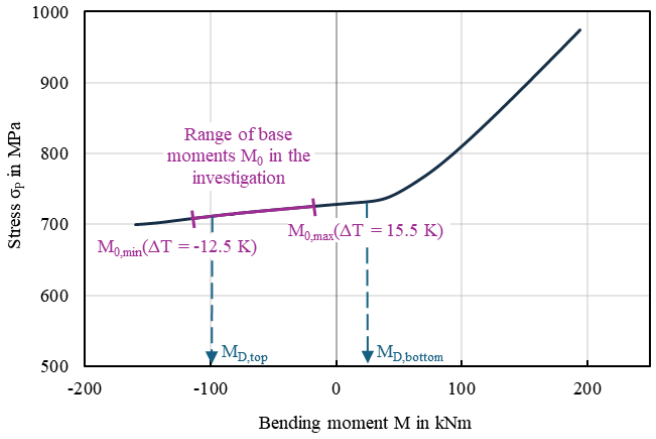

Figure 11. Moment-stress diagram for coupling joint of openLAB with moment impacts caused by applied temperature gradients.

The most extreme temperature gradients ΔT determined from all test series in Figure 10 are – 12.5 K and + 15.5 K. The range of base moments M_0 resulting from all measured temperature gradients between these values is represented as a purple section on the curve in Figure 11. The moments that lead to cracks in the cross-section M_D (exceeding the decompression point) are marked with blue arrows. $M_{D,top}$ represents the base moment that causes the cross-section to crack at the top of the bridge cross-section. $M_{D,bottom}$ represents the base moment that leads to cracking at the bottom edge. It can be seen that the calculated positive temperature gradients are not high enough to cause cracking at the bottom edge. Consequently, negative temperature gradients result in higher stress ranges in the prestressing steel and, therefore, greater partial fatigue damage $D_{\Delta T,i}$ compared to positive temperature gradients of the same absolute magnitude. This explains why the positive gradients have a positive effect on the load-bearing capacity of the structure. In this case, the coupling joint tends to crack at the upper edge of the cross-section instead of cracking at the bottom edge, as is the case with conventional prestressed bridges [5].

The variation of sampling frequency (Test No. 2.2 – 2.4), sensor density (Test No. 3.2), and local distribution of sensors (Test No. 4.2 and 4.3) have a considerably lower influence on the service life span than the period of data collection (Test No. 1.1 – 1.7). Consequently, a reduced frequency of measurements, may suffice to reliably estimate the actual temperature distribution. A lower sampling frequency reduces the amount of data collected. The impact of variations in local distribution cannot be reliably assessed in this particular case due to the limited number of sensors available. To obtain reliable results, additional temperature sensors are required, particularly within the slab of the openLAB bridge and in the edge areas of the component, where the largest gradients occur. The installation and operation of additional sensors in the openLAB is carried out in April 2025. The same evaluation methodology will be applied again with the new data generated by additional sensors to prove the representativeness and coverage of the enhanced monitoring concept.

5 CONCLUSIONS AND OUTLOOK

This study provides a methodological approach for the systematic evaluation of the monitoring concept quality applied to a bridge structure. The fatigue recalculation of the coupling joint was utilized as an example for the implementation of the sensitivity analysis concerning the temperature data. It is based on a single case study of a research bridge, which limits the statistical significance of the results. It should be mentioned that the research bridge used in this study has considerably smaller dimensions and a different structural design compared to typical prestressed concrete bridges. Consequently, the findings cannot be directly generalized to conventional prestressed bridges. The primary focus of this work is the methodology itself, which requires further testing and validation on real-world, full-scale bridges. The introduced methodology can be applied to other sensor types and failure mechanisms.

The presented evaluation of temperature data indicates that, in this particular case study, the temporal representativeness expressed by the varied period of data collection has the most impact on the fatigue calculation of the coupling joint. The lower temporal coverage expressed by the lower sampling frequency does not notably affect the results of the recalculation. Spatial coverage and spatial representativeness could not be properly evaluated in this case study due to the limited number of sensors. It is not yet possible to derive universally applicable recommendations for the design of measurement systems for coupling joints based solely on this case study. Further investigations with a greater number of sensors are required to achieve this objective.

In addition to temperature monitoring, concrete strain or prestressing steel strain ranges are usually recorded at coupling joints. To determine an appropriate holistic monitoring concept for this specific structure, investigations are also required for

DOI: 10.3217/978-3-99161-057-1-154

these measurements. The load tests that will be performed on the openLAB bridge in 2025 can be used to validate and update the existing FE model. The appropriate estimation of the base moment M_0 and the determination of the moment-stress curve, which describes the transition of the coupling joint from Mode I to Mode II, play a key role in this context.

In summary, further research on the quality of monitoring concepts has the potential to refine existing monitoring approaches and to provide a more accurate assessment of impacts at coupling joints of prestressed concrete bridges. The quality control of monitoring concepts and data should be incorporated as a key component in relevant standards and regulations. This not only facilitates a more reliable condition assessment but also supports a potential extension of the service life of bridge structures.

ACKNOWLEDMENTS

This research was funded by the Federal Ministry for Digital and Transport within the research project ANYTWIN (Standardizing Monitoring Based Safety Assessments of Bridges and the Integration into Digital Twins, grant number: 01F2248B) and by the German Research Foundation (DFG) as part of the Priority Program 2388 (SPP 2388) “Hundred plus – Extending the Lifetime of Complex Engineering Structures through Intelligent Digitalization” (project number: 501808860). This article represents the opinions of the authors and does not mean to represent the position or opinions of the funding entities.

REFERENCES

[1] BASt, Brückenstatistik (Bundestfernstraßen), https://www.bast.de/DE/Ingenieurbau/Fachthemen/brueckenstatistik/bruecken_hidden_node.html, 2024.

[2] Treacy, M. A.; Brühwiler, E., A direct monitoring approach for the fatigue safety verification of construction joint details in an existing post-tensioned concrete box-girder bridge in: Engineering Structures 88, p. 189–202, https://doi.org/10.1016/j.engstruct.2015.01.036, 2015.

[3] Geißler, K., Handbuch Brückenbau, first edition, Wilhelm Ernst & Sohn, Berlin, Germany, https://onlinelibrary.wiley.com/doi/book/10.1002/9783433603437, 2014.

[4] Seible, F., Coupling Joints of Prestressing Tendons in Continuous Post-Tensioned Concrete Bridge in: Structures and foundations, Transportation Research Record, issue number 1044, p. 43-49, https://onlinepubs.trb.org/Onlinepubs/trr/1985/1044/1044-007.pdf, 1986.

[5] König, G.; Gerhard, H.-C., Beurteilung der Betriebsfestigkeit von Spannbetonbrücken im Koppelfugenbereich unter besonderer Berücksichtigung einer möglichen Rißbildung in: Deutscher Ausschuss für Stahlbeton, issue number 370, Wilhelm Ernst & Sohn, Berlin, Germany, p. 85-123, 1986.

[6] Zilch, K.; Zehetmaier, G.; Gläser, C., Beton Kalender: Brücken und Parkhäuser - Ermüdungsnachweis bei Massivbrücken, Wilhelm Ernst & Sohn, Berlin, Germany, 2004.

[7] Maibaum, M.; Li, Z.; Puttkamer, L., ANYTWIN - Identifikation wesentlicher Einflussparameter für – auf Grundlage von Auswertungen des Nachrechnungsbestandes – ausgewählte Versagensmechanismen in: Technische Akademie Esslingen 6. Brückenkolloquium, Narr Francke Attempto Verlag GmbH + Co. KG, Tübingen, Germany, 2024.

[8] Buba, R., Zur stochastischen Zuverlässigkeit bestehender Spannbetonbrücken gegen Ermüdung, Technische Universität München, Germany, 2005.

[9] Zilch, K. et al., Bericht zum Forschungsprojekt 15.0652: Integration der Handlungsanweisungen "Spannungsrisskorrosion" und "Koppelfugen" in die Nachrechnungsrichtlinie, Heft B 186, Bergisch Gladbach, Germany, https://bast.opus.hbz-nrw.de/opus45-bast/frontdoor/deliver/index/docId/2747/file/B186+Gesamtversion+BF.pdf, 2023.

[10] BASt, Richtlinie zur Nachrechnung von Straßenbrücken im Bestand (Nachrechnungsrichtlinie), Bergisch Gladbach, Germany, https://www.bast.de/DE/Publikationen/Regelwerke/Ingenieurbau/Entwurf/Nachrechnungsrichtlinie-Ausgabe-5_2011.html, 2011.

[11] Fischer, O. et al., Nachrechnung von Betonbrücken - systematische Datenauswertung nachgerechneter Bauwerke, Bd. B 124, Bergisch Gladbach, Germany, https://bast.opus.hbz-nrw.de/files/1609/B124_barrierefreies_ELBA_PDF.pdf, 2016.

[12] BASt, 1. Ergänzung zur Richtlinie zur Nachrechnung von Straßenbrücken im Bestand (Nachrechnungsrichtlinie), Bergisch Gladbach, Germany, https://www.bast.de/DE/Publikationen/Regelwerke/Ingenieurbau/Entwurf/1_Ergaenzung-Nachrechnungsrichtlinie-Ausgabe-5_2011.html, 2015.

[13] Kiureghian, A. D.; Ditlevsen, O., Aleatory or epistemic? Does it matter? in: Structural Safety 31, H. 2, p. 105–112. https://doi.org/10.1016/j.strusafe.2008.06.020, 2009.

[14] Winnewisser, N. R. et al., How to Determine the Level of Epistemic Uncertainty and Exclude Faulty Sensors in Structural Health Monitoring Systems in: IABSE Symposium, Tokyo 2025: Environmentally Friendly Technologies and Structures: Focusing on Sustainable Approaches. Tokyo, Japan. International Association for Bridge and Structural Engineering (IABSE) Zurich, Switzerland, p. 745–752, 2025.

[15] Richter, B. et al., Intermediately discretized extended α -level-optimization – An advanced fuzzy analysis approach in: Advances in Engineering Software, volume 202. https://doi.org/10.1016/j.advengsoft.2025.103865, 2025.

[16] Zilch, K.; Hennecke, M.; Buba, R., Kombinationsregeln für Ermüdung - Untersuchung der Grundlagen für Betriebsfestigkeitsnachweise bei Spannbetonbrücken, Bundesministerium für Verkehr, Bau- und Wohnungswesen, Forschung Straßenbau, volume 824, Bonn, Germany, 2001.

[17] Sanio, D. et al., Bauwerksmessungen versus Rechenkonzepte zur Beurteilung von Spannstahlermüdung in Betonbrücken in: Bautechnik, issue number 95, H. 2, p. 99–110, https://doi.org/10.1002/bate.201700092, 2018.

[18] Penka, E., Beurteilung der Ermüdungssicherheit von Koppelfugenquerschnitten bestehender Spannbetonbrücken durch Langzeitmessungen, Technische Universität München, Germany, 2004.

[19] BASt, Erfahrungssammlung Monitoing für Brückenbauwerke - Dokumentation 2021. Fachverlag NW in der Carl Ed. Schünemann KG, Bergisch Gladbach, Germany, https://bast.opus.hbz-nrw.de/files/2901/B197+Gesamtversion+BF.pdf, 2024.

[20] Weiher, H.; Runtemund, K.; Ullerich, C. (2015) Monitoringbasierter Nachweis der Spannstahlermüdung an den Koppelfugen der Köhlbrandbrücke in: Beton- und Stahlbetonbau, issue number 110, H. 8, p. 529–538. https://doi.org/10.1002/best.201500029, 2015.

[21] Herbers, M. et al., openLAB – Eine Forschungsbrücke zur Entwicklung eines digitalen Brückenzwillings in: Beton- und Stahlbetonbau, issue number 119, H. 3, p. 169–180. https://doi.org/10.1002/best.202300094, 2024.

[22] Richter, B. et al., Monitoring of a prestressed bridge girder with integrated distributed fiber optic sensors in: Procedia Structural Integrity, issue number 64, p. 1208–1215, https://doi.org/10.1016/j.prostr.2024.09.168, 2024.

[23] Krohn, S., Messwertgestützte Ermüdungsnachweise an bestehenden Straßenbrücken – Entwerfen und Konstruieren Stahlbau, Shaker Verlag, Aachen, Germany, 2014.

[24] Miner, M. A., Cumulative Damage in Fatigue in: Journal of Applied Mechanics 12, H. 3, p. 159-164. https://doi.org/10.1115/1.4009458, 1945.

[25] Foken, T. (2021) Springer Handbook of Atmospheric Measurements, first edition, Cham: Springer International Publishing, University of Bayreuth Bayreuth, Germany, https://doi.org/10.1007/978-3-030-52171-4, 2021.

[26] VDI 3786, Umweltmeteorologie Umweltmeteorologie- Meteorologische Messungen - Grundlagen – Environmental meteorology - Meteorological measurements - Fundamentals. DIN Media GmbH, Berlin, Germany, 2024.

[27] Meteoblue, Wetterarchiv Bautzen für Juli 2024 – Saxony, Germany, https://www.meteoblue.com/de/wetter/historyclimate/weatherarchive/bautzen_deutschland_2951881?fcstlength=1m&year=2024&month=7 [last access on 9 April 2025].